molecular pharmaceutics

pubs.acs.org/molecularpharmaceutics Article

Characterizing Drug−Polymer Interactions in Aqueous Solution with Analytical Ultracentrifugation

Kweku K. Amponsah-Efah, Borries Demeler, and Raj Suryanarayanan*

Cite This: https://dx.doi.org/10.1021/acs.molpharmaceut.0c00849 Read Online

ABSTRACT: We present a new approach for characterizing drug−polymer interactions in aqueous media, using sedimentation velocity analytical ultracentrifugation (AUC). We investigated the potential interaction of ketoconazole (KTZ), a poorly water-soluble drug, with polyacrylic acid (PAA) and a polyvinyl caprolactam−polyvinyl acetate−polyethylene glycol graft copolymer (Soluplus) in aqueous buffers. The effect of the polymer on the sedimentation coefficient of the drug was the observable metric. The drug alone, when subjected to AUC, exhibited a very narrow sedimentation peak at 0.2 Svedberg (S), in agreement with the expectation for a monomeric drug with a molar mass < 1000 Dalton. Conversely, the neat polymers showed broad profiles with higher sedimentation coefficients, reflecting their larger more heterogeneous size distributions. The sedimentation profiles of the drug−polymer mixtures were expectedly different from the profile of the neat drug. With KTZ-Soluplus, a complete shift to faster sedimentation times (indicative of an interaction) was observed, while with KTZ-PAA, a split peak indicated the existence of the drug in both free and interacting states. The sedimentation profile of carbamazepine, a second model drug, in the presence of hydroxypropyl methyl cellulose acetate succinate (HPMCAS, another polymer) revealed multiple "populations" of drug−polymer species, very similar to the sedimentation profile of neat HPMCAS. The interactions probed by AUC were compared with the results from isothermal titration calorimetry. In vitro dissolution tests performed on amorphous solid dispersions prepared with the same drug−polymer pairs suggested that the interactions may play a role in prolonging drug supersaturation. The results show the possibility of characterizing drug−polymer interactions in aqueous solution with high hydrodynamic resolution, addressing a major challenge frequently encountered in the mechanistic investigations of the dissolution behavior of amorphous solid dispersions.

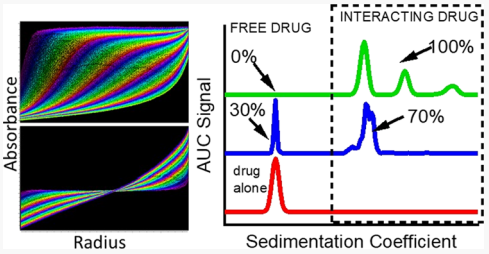

KEYWORDS: *sedimentation velocity analytical ultracentrifugation, amorphous solid dispersions, drug, polymer interactions, dissolution*

INTRODUCTION

When given orally, a solid drug must first dissolve in the gastrointestinal fluid, before being absorbed into the bloodstream.[1] Unfortunately, about 80% of drugs in the development pipeline are crystalline hydrophobic compounds with poor aqueous solubility.[2,3] Therefore, a key focus in pharmaceutical science research is to develop strategies that could overcome this solubility challenge.[4] One approach is to formulate amorphous solid dispersions (ASDs), wherein the drug is mixed with a polymer at the molecular level to form a homogeneous phase.[2,4,5]

One major consideration in formulating an ASD into a solid dosage form is to prevent drug crystallization during the shelf life of the product. Strong intermolecular interactions between the drug and the polymer (particularly ionic and hydrogen bonding interactions) can result in ASDs that are physically stable for timescales of pharmaceutical interest.[6−8] When the ASD is taken by the patient, supersaturated drug concentrations may be achieved in the gastrointestinal fluid.[5] To realize the solubility advantage, drug crystallization should also be prevented for a period long enough to allow absorption to occur.[2] A widely held view is that an optimum strength of the drug−polymer interaction in solution is required to maintain the desired level of supersaturation.[9−11] If the interaction is too weak, the drug may rapidly crystallize from solution. If the interaction is too strong, it is possible that the drug−polymer complex may not dissociate, and in spite of being in solution, the drug may be unavailable for absorption. Adequate characterization of the nature and strength of drug−polymer interactions in aqueous solutions therefore aids both in understanding and interpreting the in vitro drug dissolution profiles.[10] Analytical methods that can provide molecular-level information on the formation, composition, structure, size, and stability of the drug−polymer complexes are thus required.

Techniques for characterizing interactions between heterogeneous species in solution include vibrational spectroscopy (e.g., infrared and Raman), fluorescence and nuclear magnetic

Received: August 17, 2020
Revised: November 5, 2020
Accepted: November 6, 2020

resonance (NMR) spectroscopy, and isothermal titration calorimetry.[12] One-dimensional (1D) vibrational spectroscopic techniques utilize shifts and general changes in characteristic vibrational bands of functional groups of the drug or polymer to indicate hydrogen bonding or ionic interactions.[7,13] The congested nature of the 1D spectra, with numerous overlapping vibrational modes, poses a significant challenge in making unambiguous peak assignments.[7] Moreover, the broad infrared absorbance band from water, especially in the 3000 cm^{-1} region, occludes signals from functional groups of interest, making it impossible to observe spectral changes of drugs in aqueous solutions.[7,13−15] Even though Raman spectroscopy is transparent to water, the signals from poorly soluble drugs tend to be very weak with high fluorescence backgrounds.

As an advancement over 1D spectroscopy, two-dimensional (2D) NMR methods provide more reliable information on drug−polymer interactions. In 2D nuclear Overhauser effect spectroscopy (NOESY), resonances are spread along multiple axes, giving a frequency correlation spectrum.[16] If the drug and polymer are within 5 Å of each other in solution, cross peaks will develop indicating interactions.[11,17,18] Interactions in solution can also be indirectly probed with diffusion measurements (via the principle of codiffusion).[19−21] A reduction in drug diffusivity in the presence of a polymer is often indicative of an interaction. Of the several solute diffusion measurement techniques (e.g., dynamic light scattering, fluorescence correlation spectroscopy, asymmetric flow field-flow fractionation, or NMR diffusion), only two-dimensional diffusion ordered spectroscopy (2D DOSY) has been successfully adapted for this application. DOSY allows simultaneous spectroscopic separation of the diffusion coefficients of heterogeneous species in solution (in a sense, reminiscent of chromatography).[17,18,22]

A significant barrier to the use of all these techniques stems from the weak signal of the drug−polymer systems in aqueous media. NMR, in particular, inherently has a lower sensitivity than many other spectroscopic methods.[23] Similarly, the need for very high drug concentrations almost entirely precludes the use of isothermal titration calorimetry (ITC).[24] While organic solvents can be used, interactions probed in such systems do not reflect interactions in aqueous solution.[25] Other techniques that can address the challenge of poor signal sensitivity in aqueous media must therefore be explored.

Analytical ultracentrifugation (AUC) is a powerful fractionation-based technique used extensively to characterize the hydrodynamic and thermodynamic properties of biomacromolecules (e.g., proteins), colloidal systems, and nanoparticles.[26−28] AUC measures sedimentation and diffusion coefficients from which the size, density, and shape of heterogeneous species in solution can be obtained.[29] Detection systems based on UV−visible absorbance, fluorescence, or interference optics make this technique amenable to a wide range of applications. The high sensitivity of the detection systems is particularly valuable for analytes with low aqueous solubility. Although AUC is suitable for the study of most macromolecules, the technique suffers from low patronage in the investigation of synthetic polymers.[30,31] There are no reports on the sedimentation behavior of pharmaceutically relevant (mostly synthetic) polymers typically used in ASD formulations. It is also not known whether the interaction of such polymers with small molecule drugs in aqueous solution can be adequately measured with AUC.

In this work, we report a method to semi-quantitatively characterize drug−polymer interactions in aqueous solution using sedimentation velocity AUC. The drug sedimentation coefficient in the presence and absence of the polymer is the metric. The free drug (in this context, a small molecule with low density and molar mass less than 1000 Da) will hardly sediment. In comparison, the bulky polymer (> 10,000 Da) should sediment rapidly. We hypothesize that when the drug interacts with the polymer, the sedimentation rate of the complexed drug changes and approaches the sedimentation behavior of the neat polymer. The drug movement in the presence of the polymer can be monitored if the UV−vis spectrum of the drug exhibits pronounced absorption in a wavelength region where the polymer does not absorb. This new AUC-based method would be analogous to the codiffusion method used for characterizing drug−polymer interactions in two-dimensional DOSY.[17,22]

We tested this method with two model hydrophobic drugs—carbamazepine (CBZ, an antiepileptic) and ketoconazole (KTZ, an antifungal)—and three polymers. The structures are shown in Figure 1, and the reasons for selecting each drug−polymer pair are given in the Experimental Section.

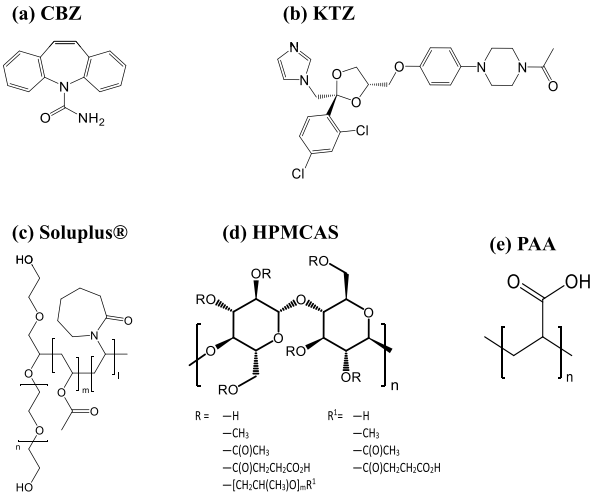

Figure 1. Structures and average molecular weights (M_w) of the drugs and polymers. (a) carbamazepine (CBZ), 236 Da, (b) ketoconazole (KTZ), 531 Da, (c) polyvinyl caprolactam—polyvinyl acetate—polyethylene glycol graft copolymer (Soluplus), 115,000 Da (ref 37), (d) hydroxypropyl methyl cellulose acetate succinate (HPMCAS), 17,000 Da (ref 41), and (e) polyacrylic acid (PAA), 1,033,000 Da.

Our main objective is to evaluate the potential utility of sedimentation velocity AUC to characterize drug−polymer interactions in aqueous media. We also compared the results of the AUC method to interactions probed via ITC. Finally, the possible effects of the interactions on the in vitro dissolution performance of ASDs were discussed.

EXPERIMENTAL SECTION

Selection of Model Systems. Three drug−polymer pairs were used in this study: (i) ketoconazole (KTZ) and poly acrylic acid (PAA), (ii) ketoconazole and Soluplus, and (iii) carbamazepine (CBZ) and hydroxypropyl methyl cellulose acetate succinate (HPMCAS). The structures are shown in Figure 1.

In ASDs, the carboxylic acid groups of PAA, a linear polymer, were shown to interact with the imidazole nitrogen of

https://dx.doi.org/10.1021/acs.molpharmaceut.0c00849
Mol. Pharmaceutics XXXX, XXX, XXX−XXX

Table 1. Solvents and Solution Concentrations Used in the AUC Experiments

sample	pH of solvent	[drug alone], mg/mL	[polymer alone], mg/mL	[(drug) + polymer mixture], mg/mL	drug/polymer ratio (by weight)
ketoconazole and PAA	1.1	0.25	0.5000	(0.25) + 0.50	1:2
ketoconazole and Soluplus	1.1	0.25	0.0625	(0.16) + 0.33	1:2
carbamazepine and HPMCAS	6.8	0.04	4.0000[a]	(0.04) + 4.00	1:100

[a]Experiments at lower polymer concentrations yielded qualitatively similar profiles.

KTZ.[8] The strong (ionic and hydrogen bonding) interactions translated to a pronounced resistance to drug crystallization, following storage of the KTZ−PAA dispersions in both glassy and supercooled states.[32,33] Our preliminary investigations (using 2D H^1H^1 NOESY and 2D DOSY) also showed that the drug−polymer interactions persisted in aqueous media.[34,35] Soluplus, the second model polymer, is a commercial polyvinyl caprolactam—polyvinyl acetate—polyethylene glycol graft copolymer that was specifically designed with amphiphilic groups for ASD formulation.[36,37] It forms micelles in water, conferring the ability to enhance the solubility of hydrophobic compounds.[37] Having no ionizable functional groups, ionic interactions with KTZ would be unlikely. Hydroxy propyl methyl cellulose acetate succinate (HPMCAS, the third polymer) is widely used in ASD formulations and facilitates the formation of stable supersaturated solutions.[10,38] Interaction of HPMCAS with CBZ in a dry solid form was recently characterized.[39] Furthermore, with NMR (2D NOESY and saturation transfer difference) experiments, it was shown that hydrophobic-driven associations between CBZ and HPMCAS exist in aqueous buffers.[11] The interaction was correlated with a reduction in carbamazepine recrystallization from supersaturated solutions.[40] The three drug−polymer pairs, KTZ−PAA, KTZ−Soluplus, and CBZ−HPMCAS, were therefore expected to provide different types of interactions in solution.

Materials. Carbamazepine (Sigma, USA), ketoconazole (Laborate Pharmaceuticals, Haryana, India), Soluplus (BASF, USA), HPMCAS, HF grade (Ashland, USA), and PAA (Sigma, USA) were used as received (Figure 1). All reagents and chemicals used to prepare the buffers and ASDs were of analytical grade.

Preparation of Amorphous Solid Dispersions. ASDs with 33% w/w drug loading were prepared by solvent evaporation. For each system, the drug and the polymer were individually dissolved in appropriate organic solvents (KTZ, Soluplus, PAA, and HPMCAS-HF in methanol; CBZ in ethanol). The solutions were combined and the solvent rapidly evaporated at 50 °C under a reduced pressure (IKA-HB10 digital system rotary evaporator, Werke GmbH and Co., Staufen, Germany). The solid dispersions were further dried at room temperature for 24 hours to remove any residual solvent, lightly ground using a mortar and a pestle in a glovebox (RH < 5%), sifted (250 μm pore size), and stored at −20 °C in desiccators containing anhydrous calcium sulfate before use. All ASDs prepared were found to be amorphous when characterized by powder X-ray diffraction [model D8 ADVANCE; Bruker AXS, Madison, WI, using Cu Kα radiation (40 kV × 40 mA) over an angular range of 5−35° 2θ with a step size of 0.05° and a dwell time of 0.5 s].

Preparation of Buffers and Solutions. Phosphate buffer (pH 6.8; 50 mM monobasic potassium phosphate and 22.4 mM sodium hydroxide) and hydrochloric acid buffer (pH 1.1; 106 mM hydrochloric acid and 50 mM potassium chloride) were used. Separate stock solutions of drug (up to 1 mg/mL) and polymer (∼15 mg/mL) were prepared by dissolving an accurately weighed amount of material in the buffer followed by filtration (0.45 μm pore filter). Aliquots of the stock solutions were pipetted into a vial and diluted with the buffer to obtain solutions with the required final compositions for ITC and AUC experiments (details in Table 1). The pH of all samples (drug solutions, polymer solutions, or their mixtures) did not differ by more than ±0.1 units of the desired value.

UV−vis Spectroscopy. UV/visible absorbance spectra were recorded in the 200−600 nm range (Cary 100 Bio, Agilent Technologies) using a quartz cuvette with a path length of 1 cm.

Analytical Ultracentrifugation. Concentrations of solutions (i.e., neat drug, neat polymer, and drug−polymer mixtures) as well as solvents used in each case are summarized in Table 1. Concentrations were chosen such that an optical density of ∼0.6 would be obtained at the desired wavelength of detection for the AUC experiments.

KTZ, PAA, and Soluplus experiments were performed at the Center for Analytical Ultracentrifugation of Macromolecular Assemblies at the University of Texas Health Science Center at San Antonio using an analytical ultracentrifuge (Optima AUC, Beckman Coulter, Indianapolis, IN) equipped with multiwavelength UV−visible detection (absorbance optics). Samples were placed into Epon centerpieces with quartz windows and measured at 20 °C, 45000 rpm using an An50Ti rotor. CBZ and HPMCAS experiments were performed at the Canadian Center for Hydrodynamics at the University of Lethbridge, Alberta, Canada. Samples were placed into titanium centerpieces (Nanolytics Instruments, Potsdam, Germany) with sapphire windows and measured at 20 °C, 60,000 rpm using an An60Ti rotor. Approximately 500 scans were collected for each wavelength. Data analyses were carried out with standard methods implemented in the UltraScan III software[42,43] using the two-dimensional spectrum analysis (2DSA)[44] coupled with Monte Carlo analysis[45] and the parametrically constrained spectrum analysis (PCSA).[46] Briefly, these methods model sedimentation velocity data with linear combinations of finite element solutions of the Lamm equation[47] to obtain sedimentation and diffusion coefficients (s and D values, respectively). The 2DSA−Monte Carlo analysis was used to obtain an unconstrained sedimentation/diffusion profile of the hydrodynamic parameter space. The 2DSA analysis was performed with simultaneous removal of time and radially invariant noise contributions. The data were further refined using PCSA. PCSA solutions were coupled with Monte Carlo analysis to determine confidence limits for the determined parameters. Computationally intensive calculations were carried out on high-performance supercomputing platforms. Sedimentation coefficient values were standardized to water at 20 °C ($s_{20,w}$). The profiles were normalized by dividing each data point in the original

https://dx.doi.org/10.1021/acs.molpharmaceut.0c00849
Mol. Pharmaceutics XXXX, XXX, XXX−XXX

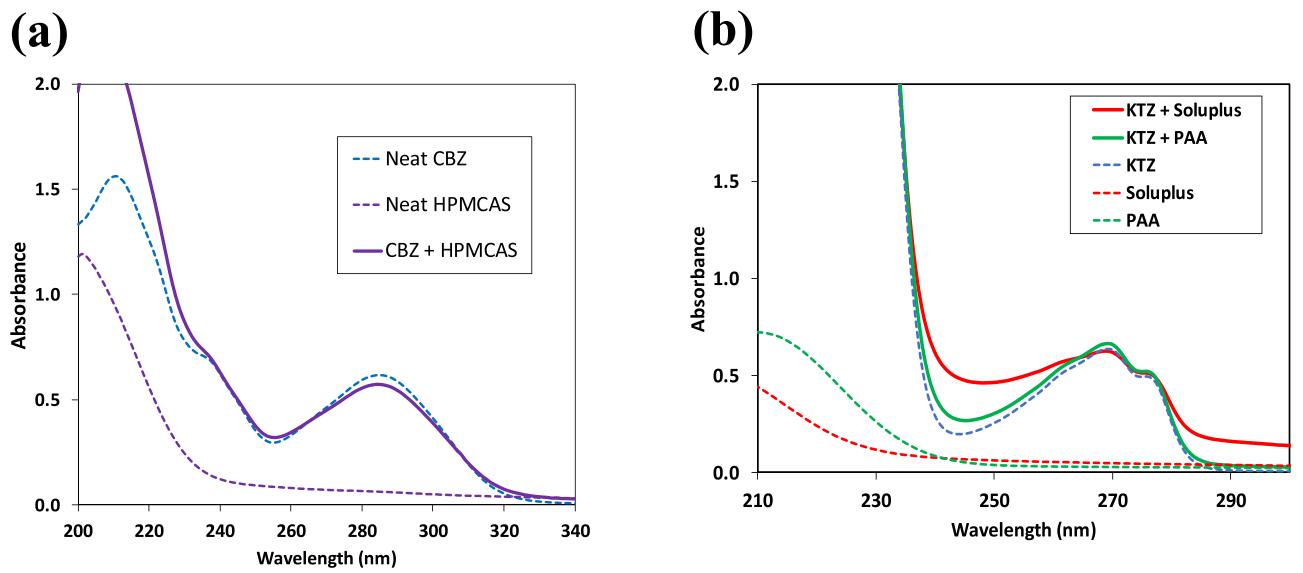

Figure 2. UV absorbance spectra of neat drugs, neat polymers, and (drug + polymer) mixtures.(a) Carbamazepine alone, HPMCAS alone, and the (CBZ + HPMCAS) mixture. (b) Ketoconazole alone, PAA alone, Soluplus alone, the (KTZ + PAA) mixture, and the (KTZ + Soluplus) mixture. Solute concentrations and solvent systems are listed in Table 1.

distribution by the maximum dC/ds data point so that the peak maximum for each distribution was equal to 1.

Isothermal Titration Calorimetry (ITC). KTZ solution (20 mg/mL) was prepared in a buffer (pH 1.1 ± 0.1) and filtered (0.45 μm PTFE) immediately before each ITC experiment. Solutions of PAA (5 mg/mL) and Soluplus (5 mg/mL) were also prepared in the same buffer (pH 1.1 ± 0.1).

A microcalorimeter (MicroCal Auto-ITC$_{200}$ system, Malvern Instruments, MA), which has a 200 μL sample cell and an identical reference cell, was used. The drug solution in the syringe was sequentially injected into the polymer solution within the sample cell at a constant stirring rate of 750 rpm. The temperature was maintained at 25 °C. The first injection was a 0.4 μL aliquot to remove the effect of solute diffusion across the syringe tip during the equilibration period. Subsequently, 4 μL injections were made into the sample cell. The duration of each injection was 20 s, and the time interval between successive injections was 180 s. The run time was extended by performing experiments in an automated "continued injection" mode, wherein when full, 30 μL of solution was withdrawn from the sample cell to make room for more sequential injections of the titrant. This process of withdrawing solution from the sample cell and continuing the titrations was repeated for up to four experiments. Individual experiments were concatenated using the Microcal origin concat (add-on) software. Data processing, integration, and analysis were carried out with the AFFINImeter software.[48]

Powder in Vitro Dissolution. Dissolution tests under nonsink conditions were performed with a USP Apparatus II (Varian 705 DS, Agilent Technologies, Santa Clara, CA). Each sample, containing 250 mg of drug, was dispersed in 250 mL of a dissolution medium (pH 6.8 buffer) set at 37 °C and stirred at a paddle speed of 100 rpm. Aliquots (2 mL) were withdrawn at each time point, filtered (0.45 μm pore size, Whatman PP), and diluted appropriately with methanol. The drug concentration in the filtrate was determined by high-performance liquid chromatography (HPLC; Nexera XR system, Shimadzu, Japan).

Chromatographic separation was performed using a reversed-phase column (Zorbax Eclipse XDB-C18, 4.6 x 150 mm, 5 μm, Agilent, USA). The mobile phase consisted of 2.55 g of tetrabutylammonium hydrogen sulfate dissolved in 750 mL of water and diluted to 1000 mL with acetonitrile. The flow rate was 1 mL/min at 30 °C. Injection volumes, detection wavelengths, and retention times were, respectively, 20 μL, 223 nm, and 4 min for KTZ and 5 μL, 230 nm, and 14 min for CBZ. Drug concentrations were calculated from linear calibration curves generated over a concentration range of 4−400 μg/mL.

RESULTS AND DISCUSSION

In general, upon dissolution of an ASD, the three main species that may exist in the solution are: (i) free drug, (ii) free polymer, and (iii) various types of drug−polymer aggregates or complexes.[10] Both free and complexed drug contribute to the total drug concentration measured via in vitro dissolution tests.[10] Any technique that can independently monitor the differing rates of solute transport (e.g., diffusion and sedimentation) and/or the relative amounts of each of these species in solution can, in principle, provide a measure of the drug−polymer interactions. This formed the basis for the experimental design.

In a typical sedimentation velocity AUC experiment, the dissolved solute within a sample cell is exposed to a high centrifugal field induced by the spinning of the centrifuge rotor. The solute transport is tracked using an optical detection system (in this case, UV multiwavelength absorbance optics) that measures the concentration change of the sample as a function of time and radius (see Supporting Information). The procedure for selecting UV absorbance wavelengths, which allows the sedimentation coefficient (s value) distribution of different species in solution to be monitored, is explained in the next section.

Wavelength Selection for Analytical Ultracentrifugation. Utilizing absorbance optics, the first step involved the examination of the UV absorbance profiles of the (i) neat drugs (ii) neat polymers, and (iii) drug−polymer mixtures.

https://dx.doi.org/10.1021/acs.molpharmaceut.0c00849
Mol. Pharmaceutics XXXX, XXX, XXX−XXX

The main consideration was to identify a wavelength region where the neat drug has a strong absorbance but where the neat polymer does not absorb. The spectra of the samples are shown in Figure 2. Solution compositions and buffers used as solvents are listed in Table 1.

Carbamazepine exhibits pronounced absorbance at wavelengths <250 nm as well as a peak at 285 nm (Figure 2a, blue dashed profile). The AUC optics can be tuned to any wavelength at which the drug absorbs to observe the sedimentation of the neat drug. The neat polymer HPMCAS, on the other hand, only absorbs significantly at wavelengths <250 nm (Figure 2a, violet dashed line profile) such that its sedimentation can only be monitored at wavelengths <250 nm. In the 250−330 nm wavelength region, the absorbance of the neat drug is much higher than the absorbance of the neat polymer such that the polymer does not contribute significantly to the absorbance of the drug−polymer mixture. The AUC optics can therefore be tuned to any wavelength in the 250−330 nm range to observe the migration of the drug in the presence of the polymer. The UV profiles of ketoconazole and the polymers, PAA and Soluplus, exhibit qualitatively similar characteristics (Figure 2b).

By monitoring the sedimentation profile of the drug−polymer mixture at a wavelength where only the neat drug absorbs, the sedimentation experiment becomes selective for the drug and any drug−polymer complexes formed. If the neat polymer sediments faster than the neat drug, any increase in the sedimentation coefficient of the drug within the polymer matrix will provide evidence of the drug−polymer interactions. This is the principle upon which the drug−polymer interactions were monitored. It should be noted, however, that the sedimentation profile of the free polymer within the mixture cannot be monitored.

Sedimentation Profiles of Neat Drugs and Polymers. Sedimentation profiles of the neat drugs and neat polymers are shown in Figure 3. The corresponding experimental raw data plots as well as the fitting residuals, which were mostly randomly distributed, are provided in the Supporting Information (Figures S1−S5; see AUC experimental methods for details of data analyses). When either CBZ (Figure 3a, M_w = 236 Da) or KTZ (Figure 3b, M_w = 531 Da) was examined alone, a very narrow sedimentation peak at 0.2 S was observed. Posaconazole, another drug with a slightly higher molecular weight (M_w = 701 Da), also showed a sedimentation coefficient at 0.2 S (data not shown). The identical sedimentation profiles are in excellent agreement with the expectation that monomeric molecules with low molecular weights (<1000 Dalton) hardly sediment and are at the limit of detection by AUC.[29]

The neat polymers, however, had very different sedimentation profiles. PAA, a linear polymer, was present in solution as a heterogeneous mixture sedimenting between 0 and 50 S (Figure 3c). The high molecular weight (1,031,000 Da), long chains (~14,300 monomers per chain), and a high dispersity index of 7.9 contributed to the broad, skewed sedimentation coefficient distribution. The larger aggregates between 10 and 50 S are likely from chain entanglement.[49] Soluplus, with the molecular weight an order of magnitude lower than that of PAA, had a narrower, more homogeneous size distribution (from 0 to 4 S) and a negligible number of larger aggregates (Figure 3d). Soluplus is amphiphilic, and the concentration examined was well above the reported critical micelle concentration of 0.0076 mg/mL.[37]

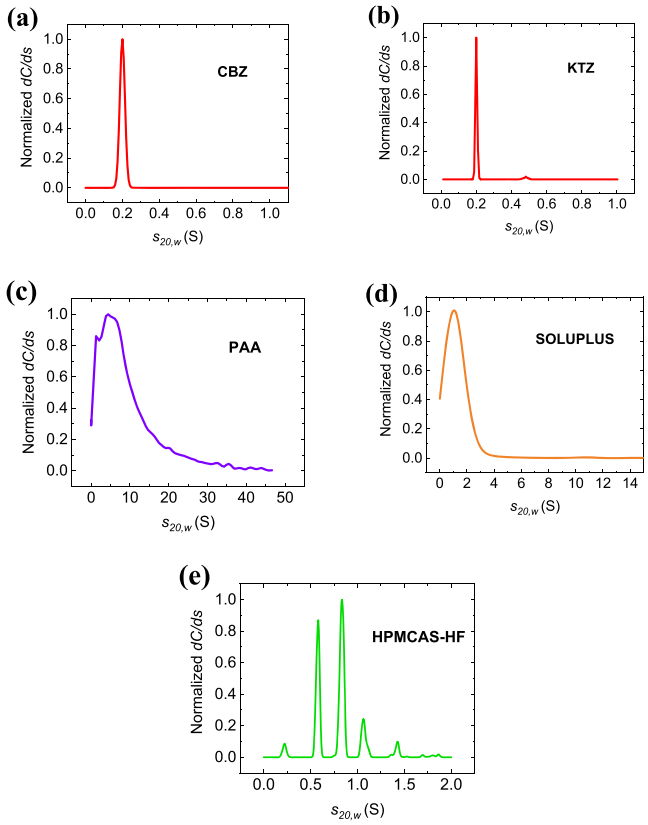

Figure 3. Sedimentation profiles of the neat drugs and neat polymers. (a) CBZ alone, observed at 315 nm, (b) KTZ alone, observed at 262 nm, (c) PAA alone, observed at 215 nm, (d) Soluplus alone, observed at 215 nm, and (e) HPMCAS alone, observed at 220 nm. Solution concentrations and solvent systems are listed in Table 1.

The sedimentation profile of neat HPMCAS, however, showed five well-defined peaks, from 0 to 2 S (Figure 3e). The molecular weight (~17,000 Da) is significantly lower than that of PAA or Soluplus, resulting in a narrower range of s values. The sharpness of the peaks, however, suggests that in solution, HPMCAS migrates as discrete, light species, which is a rather surprising observation. Of note, all polymer solutions were measured at sufficiently low concentrations to avoid nonideal sedimentation.[50−52] Because of the amphiphilic nature of HPMCAS, a widely held view is that any higher order structures in solution will be due to colloidal aggregation or gelation.[10,38] Friesen et al., using cryogenic transmission electron microscopy, characterized a range of nanometer-sized structures (mainly 10−20 nm polymer colloids and a few 70−300 nm nanoaggregates) formed by HPMCAS in an aqueous buffer (pH 6.8).[10] They posited that because HPMCAS is partially ionized at pH 6.8, the charge on the polymer allows the colloids to remain stable, while minimizing the formation of much larger aggregates.[10] Ricarte et al., however, suggested that the large species, also observed with light scattering measurements over a wide concentration range (0.01 to 9 mg/mL), were from chain coupling (i.e., covalently cross-linked chains) and not from colloidal aggregation.[53] Both scenarios could result in discrete sedimenting fractions being observed in this study. It is also possible that the different combinations of acetyl and succinoyl substituents of the cellulose backbone (the R and R^1 groups shown Figure 1d) result in polymer fractions that sediment at different speeds. If the latter explanation holds, the sedimentation profiles of neat

https://dx.doi.org/10.1021/acs.molpharmaceut.0c00849
Mol. Pharmaceutics XXXX, XXX, XXX−XXX

polymer solutions manufactured with different specifications may possibly be characteristic, allowing the use of the technique as a quality control measure. Clearly, this interesting sedimentation profile warrants further investigation.

Sedimentation Profiles of Drug−Polymer Mixtures. Sedimentation profiles of the drug−polymer mixtures, each overlaid with the profile of the corresponding neat drug, are shown in Figure 4. Experimental raw data for each sample, as well as the fitting residuals, are also provided in the Supporting Information (Figures S6−S8). For each sample, shifts to higher sedimentation coefficient values (s values) were observed, which can be attributed to the drug−polymer interactions.

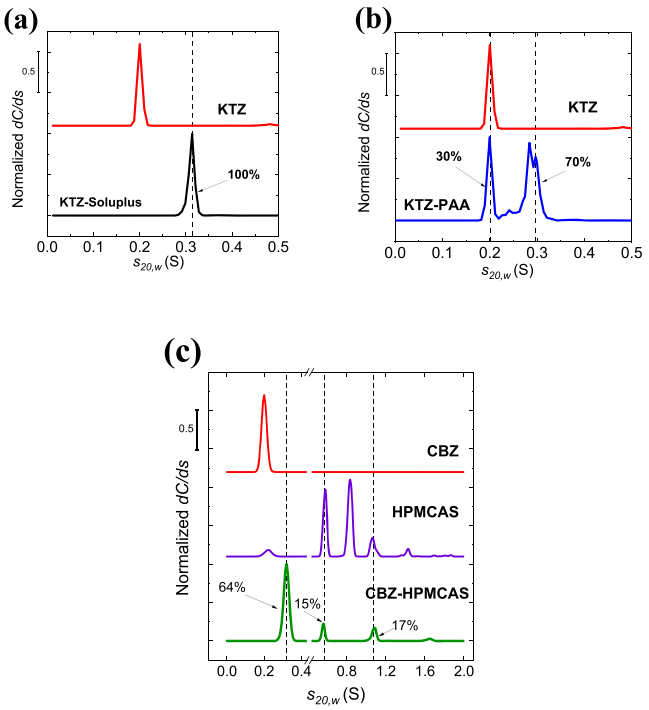

Figure 4. Sedimentation profiles of drug−polymer mixtures. (a) KTZ−Soluplus observed at 262 nm, stacked with KTZ alone. (b) KTZ−PAA observed at 262 nm, stacked with KTZ alone. (c) CBZ−HPMCAS observed at 315 nm, stacked with CBZ alone and HPMCAS alone. The peak positions of the drug−polymer mixtures are indicated with dashed vertical lines. The percentage abundance of different fractions is listed in Table 2.

The KTZ−Soluplus mixture (Figure 4a, bottom profile) showed a complete shift in s value, suggesting that the drug molecules migrate at the same rate (in a single distribution) in the presence of the polymer. For the KTZ−PAA mixture, a split peak was observed; the first peak was at 0.2 S, which matches with the peak position of neat KTZ, and the second peak was centered at 0.3 S, a faster sedimentation rate compared to the neat drug (Figure 4b). This observation suggests a mixture of free (30%, at 0.2 S) and interacting (70%, at 0.3 S) drug fractions, respectively, at the concentration level evaluated.

The sedimentation profile of the CBZ−HPMCAS system shows four peaks in the 0 to 2 S region (Figure 4c, green bottom profile). Evidently, this profile is very different from the single sharp peak of the neat drug and more closely resembles the profile of neat HPMCAS (Figure 4c, middle profile). The first peak of the drug−polymer mixture appears at 0.3 S (~0.1 S shift in s value when compared to the neat drug), indicating that there is no free drug fraction. The three additional peaks of the drug−polymer mixture, which appear at 0.6, 1.1, and 1.7 S, match the peak positions of the neat polymer. The peak positions and the corresponding peak areas for all the drug−polymer pairs are listed in Table 2. If the multiple peaks of neat HPMCAS indeed result from the diverse substituent units of the cellulose backbone, this observation would mean that CBZ preferentially partitions into different polymer fractions. The ability to quantify with high resolution the different fractions of the drug−polymer complexes is indeed a key advantage of the AUC technique.

Table 2. Peak Positions and Peak Areas for the Neat Drugs, Neat Polymers, and Drug−Polymer Mixtures

component	standardized sedimentation coefficient ($s_{20,w}$, S)	abundance (%)
neat CBZ (or KTZ)	0.2	100.0
neat Soluplus	1.2	100.0
neat PAA	4.4	100.0
neat HPMCAS	0.2	3.3
	0.6	32.7
	0.8	46.3
	1.1	12.0
	1.4	4.2
	1.8	1.5
CBZ + HPMCAS	0.3	63.9
	0.6	15.1
	1.1	17.4
	1.7	3.6
KTZ + Soluplus	0.3	100.0
KTZ + PAA	0.2	30.7
	0.3	69.3

General Inference from AUC Results. Overall, the AUC results suggest that the drugs form very weak associations with the polymers, which are much weaker than the binding interactions conventionally probed by sedimentation velocity AUC, such as ligand−protein or protein−protein interactions.[26,54] This inference is made because the magnitude of the shift in the sedimentation coefficient of the drug−polymer mixture (relative to the drug alone) is rather small. If the drug was tightly bound to the polymer, the sedimentation pattern of the drug−polymer mixture would have mirrored the sedimentation pattern of the neat polymer. The CBZ−HPMCAS system gives a close support of this expectation. However, in the KTZ−polymer systems, only subtle shifts in the drug sedimentation coefficient were observed, indicating that a weight average free versus interacting drug sedimentation is favored by the free state. The weak shifts in the s value make it impossible to perform additional analyses of the sedimentation data, which could have allowed extraction of other thermodynamic information. Nonetheless, the percent abundance of the various species, obtained from the peak areas, allows for semi-quantitative rank ordering of the interaction strengths.

Isothermal Titration Calorimetry (ITC). ITC provided an avenue to assess the energetics of the drug−polymer interactions in aqueous solution. Generally, ITC experiments require very high ligand (the drug, in this case) concentrations so as to obtain data sets optimal for the reliable determination of thermodynamic parameters.[24] This condition is typically not met for drugs with poor aqueous solubility. However, we took

https://dx.doi.org/10.1021/acs.molpharmaceut.0c00849
Mol. Pharmaceutics XXXX, XXX, XXX−XXX

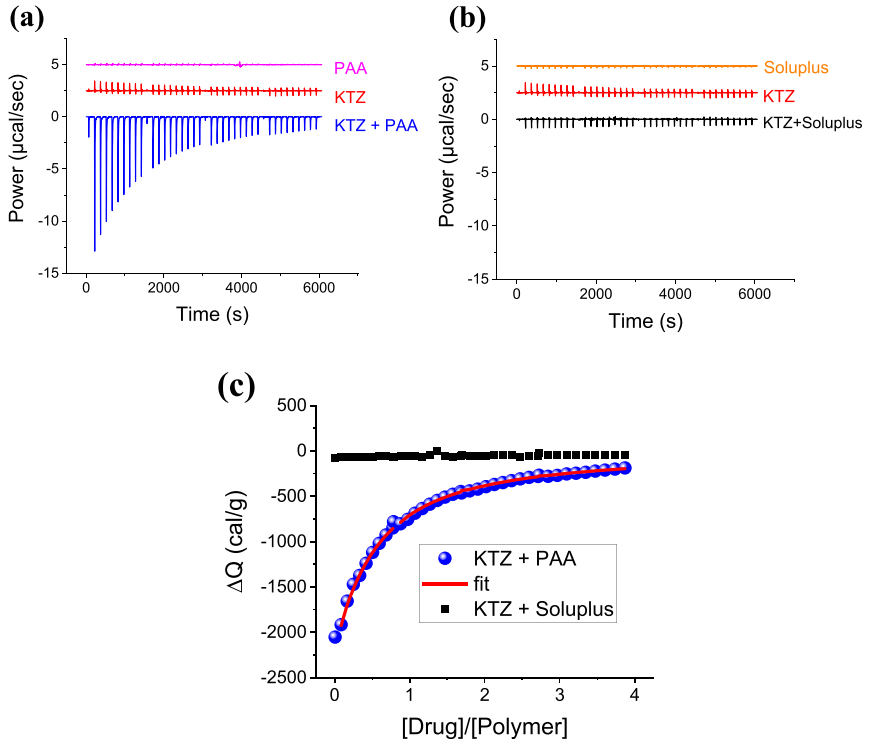

Figure 5. ITC raw data measured during the stepwise injection of KTZ (20 mg/mL) into (a) 5 mg/mL PAA and (b) 5 mg/mL Soluplus. The solvent was pH 1.1 buffer. Each panel also has the profile for the titration of the drug into plain buffer (labeled as KTZ, offset by 2.5 units on the vertical axis for clarity) and the profile for titration of buffer into the polymer solution (labeled PAA or Soluplus, offset by 5 units). (c) Overlay of the integrated heat data (ΔQ per gram of drug injected) as a function of the drug-to-polymer ratio in the sample cell (concentrations expressed in mg/mL).

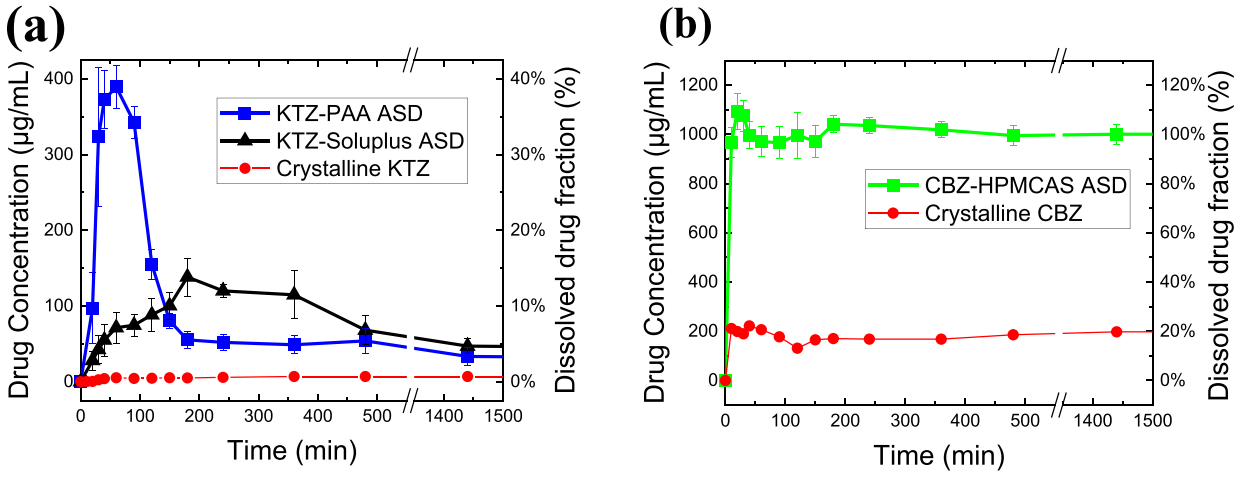

Figure 6. In vitro powder dissolution profiles of ASDs, each at 33%w/w drug loading, (a) KTZ−PAA ASD and KTZ−Soluplus ASD and (b) CBZ−HPMCAS ASD. Data points (with bars) are the arithmetic means of three replicate runs (with standard deviations).

advantage of the pH-dependent aqueous solubility of KTZ. Being a weak base (pKa values of 6.5 and 2.9), KTZ is practically insoluble at pH > 4 but highly soluble in acidic buffers (pH < 2.5; 20 °C).[55] A solution with a high drug concentration (~20 mg/mL) could thus be prepared in an acidic solvent, making it possible to perform ITC experiments. Conversely, because the aqueous solubility of CBZ is very low (<0.22 mg/mL) at all pH values, ITC experiments with CBZ in HPMCAS could not be performed.

Figure 5a shows the power compensation signals for the titration of KTZ into PAA. Exothermic peaks were initially registered, which progressively decreased in magnitude as the drug was titrated into the polymer solution. The control experiments comprising titration of the drug solution into the blank buffer or the titration of buffer into the polymer solution (respectively labeled as KTZ and PAA as shown in Figure 5a) yielded negligible heats.

The peaks obtained for the titration of the drug into the polymer were integrated to obtain the heat change (ΔQ) at each injection and then plotted as a function of the drug-to-polymer ratio in the sample cell (Figure 5c). The shape of the curve obtained for KTZ-PAA is typical for binding interactions with weak affinity (association constants less than 10^4 M^{-1}).[24,56] An overall enthalpy change of −10.2 kcal/g was

https://dx.doi.org/10.1021/acs.molpharmaceut.0c00849
Mol. Pharmaceutics XXXX, XXX, XXX−XXX

Table 3. Dissolution Test Results (±Standard Deviation, n = 3)

	sample	C_{max} (μg/mL)	t_{max} (min)	area under curve, $t_{0 \rightarrow 8hr}$ (μg/mL·min)	dissolution enhancement factor[a], $t_{0 \rightarrow 8hr}$	area under curve, $t_{0 \rightarrow 24hr}$ (μg/mL·min)	dissolution enhancement factor[a], $t_{0 \rightarrow 24h}$
1	CBZ crystalline	221	40	82722	**1.0**	266533	**1.0**
2	CBZ−HPMCAS ASD	1093 (±71)	20	480567 (±15721)	**1.8 (±0.1)**	1438455 (±48,398)	**5.4 (±0.2)**
3	KTZ crystalline	7	360	2602	**1.0**	9163	**1.0**
4	KTZ−Soluplus ASD	138 (±25)	180	46197 (±7985)	**5.1 (±0.9)**	101449 (±19675)	**11.1 (±2.1)**
5	KTZ−PAA ASD	389 (±28)	60	53579 (±4843)	**5.8 (±0.5)**	95380 (±12,106)	**10.4 (±1.3)**

[a]Dissolution enhancement factor = (area under curve of the sample)/(area under curve of the crystalline drug).

obtained when the data were analyzed with the independent sites fitting method,[48] indicating an enthalpy-driven interaction. The titration of KTZ into Soluplus (Figure 5b), however, showed very weak peaks (~0.5 μcal/sec) of the same magnitude as the peaks from the drug dilution experiment, resulting in a flat, featureless binding isotherm (Figure 5c).

The ITC experiments (via the shape of the binding isotherm) confirm the inference from the AUC experiments that drug−polymer interactions are generally very weak. The KTZ−PAA exothermic heats are most likely from electrostatic interactions between the carboxylic acids of the polymer (pKa 4.5) and the ionizable imidazole groups of the drug (see Figure 1). Soluplus on the other hand has no ionizable functional groups or hydrogen bond donors (except the end groups). Thus, ionic or hydrogen bonding interactions of KTZ with Soluplus would be unlikely, providing a reasonable explanation for the observation that there were no heats released or absorbed.

Dissolution of Amorphous Solid Dispersions. The in vitro performance of ASDs prepared by solvent evaporation was evaluated with powder dissolution studies conducted in pH 6.8 buffer under nonsink conditions. The dissolution profiles are shown in Figure 6, and the results are summarized in Table 3. The maximum concentration of the neat crystalline drugs recovered in solution was just about the same as the equilibrium solubility values reported in the literature (220 μg/mL for CBZ[57] and 3 μg/mL for KTZ[55] at 37 °C, pH 6.8).

The ASDs, each at a nominal drug concentration of 1000 μg/mL, resulted in substantially higher dissolved drug concentration levels, compared to the neat crystalline drugs. For the KTZ−PAA ASD (Figure 6a), a rapid surge in the drug concentration was observed (C_{max} ≈ 390 μg/mL) followed by a sharp decline to ~55 μg/mL, presumably as a result of drug crystallization. In contrast, a gradual rise in the drug concentration was observed for the KTZ−Soluplus ASD with a substantially lower C_{max} value (~140 μg/mL) even though the maximum level of supersaturation was sustained for a longer duration. The profile of the CBZ−HPMCAS ASD (Figure 6b) showed complete drug release within the first 20 min, with the supersaturation sustained for 24 h.

The composite effect of the extent and duration of supersaturation was quantified by normalizing the area under the dissolution profile of each ASD with the area under the curve of the corresponding crystalline drug. The resulting dissolution enhancement factors are listed in Table 3. The dissolution enhancement of the PAA dispersion, despite the rapid surge in the drug concentration, was about the same as the enhancement from the Soluplus dispersion over the physiologically relevant time frame (up to 8 h, ~5-fold enhancement) and even when extended to a 24 h period (~10-fold enhancement). A five-fold dissolution enhancement was obtained for the CBZ−HPMCAS dispersion in 24 h. It is worth noting that the nominal drug concentration for the CBZ−HPMCAS ASD in the dissolution vessel (1000 μg/mL) was only 4.5 times higher than the CBZ crystalline solubility. Dissolution experiments performed using a higher quantity of the ASD (nominal drug concentration of 2200 μg/mL, 10 times the crystalline solubility) yielded a qualitatively similar profile with no decline in the dissolved drug concentration beyond 24 h (data not shown).

Possible Effects of Interaction Strength on Supersaturation. The polymers used in this study are hydrophilic. Thus, the initial rate of drug release from ASDs will most likely be controlled by the rate at which the polymer dissolves in the dissolution medium.[58−60] Rapid polymer dissolution results in immediate liberation of the amorphous drug, generating supersaturated solutions, as observed for the KTZ−PAA and CBZ−HPMCAS dispersions. Additionally, PAA creates an acidic microenvironment favorable for the dissolution of the basic drug, KTZ.[61] The slower initial drug release rate from the KTZ−Soluplus dispersion, however, suggests that, despite its hydrophilic nature, the polymer possibly formed a "gel-like" matrix from which the amorphous drug slowly diffused.

Once the drug is released in solution, however, it is likely that drug−polymer interactions will play a more substantial role in sustaining the level of supersaturation.[58] When the polymer remains associated with the dissolved drug, nucleation and crystal growth (the two stages of crystallization) can be prevented.[58] It is reasonable to expect that the duration of supersaturation will be related to the fraction of drug molecules that remain associated with the polymer in solution, and this information can be obtained from the AUC sedimentation profiles.

If the drug−polymer interaction strengths revealed by AUC were to be rank-ordered, CBZ−HPMCAS (Figure 4c; 100% of drug molecules associated with the polymer, with strong shifts in s value) would be considered the strongest interacting system followed by KTZ−Soluplus (Figure 4a; 100% of drug molecules associated with polymer, but not as strong a shift in s value). The KTZ−PAA system (Figure 4b) would be considered the weakest interacting since 30% of the drug remained free.

Interestingly, the duration of maximum supersaturation observed for the dissolution profiles of ASDs appears to follow a similar trend. In the CBZ−HPMCAS ASD, supersaturation was sustained far beyond 24 h; for KTZ−Soluplus, supersaturation was sustained for up to 6 hours, and for KTZ−PAA, supersaturation was sustained for just ~2 h. The similarity in

https://dx.doi.org/10.1021/acs.molpharmaceut.0c00849
Mol. Pharmaceutics XXXX, XXX, XXX−XXX

the trends may be merely coincidental since the conditions for the AUC experiments were not identical to the conditions for the in vitro dissolution tests. Particularly, while the dissolution tests were performed in a neutral medium (pH 6.8), the AUC experiments for the ketoconazole systems were performed under acidic conditions (pH 1.1, in order to increase the signal strength and ensure solution stability). Furthermore, the ionization behaviors of both ketoconazole and PAA are pH dependent,[49,55] which could potentially affect the drug−polymer interaction strengths and dissolution profiles. Ketoconazole in acidic solvents is positively charged but substantially uncharged in neutral conditions. PAA, on the other hand, remains uncharged with a somewhat globular conformation in acidic solvents but negatively charged with a more extended conformation in neutral solvents.[49] It would therefore be speculative to unequivocally attribute the trends in dissolution profiles observed in the current study solely to the interaction strengths probed by the AUC technique. Nonetheless, AUC adds a new dimension, that is, sedimentation metrics and other hydrodynamic parameters, to investigations aimed at unraveling the impact of drug−polymer interactions on dissolution enhancement. With other systematic studies performed on a wider range of drug−polymer systems, a clearer picture is likely to emerge about the relevance of the nature and the strength of interactions on the dissolution enhancement of ASDs.

CONCLUSIONS

We have presented a novel approach for characterizing drug−polymer interactions in aqueous solution using sedimentation velocity AUC with multiwavelength UV detection. The uniqueness and strength of the technique stem from the ability to track the sedimentation behavior of the drug in the presence and absence of the polymer. We analyzed drug−polymer pairs that were expected to present different types of interactions in aqueous solution based on their chemistry. In each case, the sedimentation coefficient (s value) of the drug−polymer complex increased, compared to the sedimentation of the neat drug, suggesting drug−polymer interactions.

The results reveal several advantages of using AUC to provide fundamental information on drug−polymer association patterns. First, there is a possibility of teasing out and quantifying the free versus interacting fractions of drug in the drug−polymer mixtures. Higher interacting drug fractions are very likely to increase the duration of supersaturation. Second, for polymers with multimodal sedimentation profiles, there is a possibility of quantifying the amount of drug that partitions into different polymer "populations". The latter will be particularly beneficial for characterizing functionalized polymers designed to interact with specific parts of drug molecules, an approach commonly used for controlled-release purposes. Third, for poorly soluble drugs that possess strong chromophores, the high sensitivity of ultraviolet absorption makes it possible to investigate interactions directly in aqueous buffers, without the need for organic cosolvents or extrinsic tags and labels. Finally, the sedimentation profiles of the neat polymers in this study were unique, indicating that AUC protocols could be refined and adopted for routine quality control testing of pharmaceutical polymers. With adequate scientific attention, AUC could be a versatile tool for physicochemical characterization of ASDs.

ASSOCIATED CONTENT

Supporting Information

The Supporting Information is available free of charge at https://pubs.acs.org/doi/10.1021/acs.molpharmaceut.0c00849.

Brief principle of analytical ultracentrifugation and AUC experimental raw data and fitting residuals for all samples (PDF)

AUTHOR INFORMATION

Corresponding Author

Raj Suryanarayanan − *Department of Pharmaceutics, University of Minnesota, Minneapolis, Minnesota 55455, United States*; orcid.org/0000-0002-6322-0575; Email: surya001@umn.edu

Authors

Kweku K. Amponsah-Efah − *Department of Pharmaceutics, University of Minnesota, Minneapolis, Minnesota 55455, United States*

Borries Demeler − *Department of Chemistry and Biochemistry, University of Lethbridge, Lethbridge, Alberta T1K 3M4, Canada*

Complete contact information is available at: https://pubs.acs.org/10.1021/acs.molpharmaceut.0c00849

Author Contributions

The manuscript was written through contributions of all authors. All authors have given approval to the final version of the manuscript.

Notes

The authors declare no competing financial interest.

ACKNOWLEDGMENTS

This work was supported by the William and Mildred Peters endowment fund (to R.S.), an NSF-GOALI grant NSF-CMMI-1662039 (to R.S.), an NIH grant GM120600 (to B.D.), and a NSF grant NSF-ACI-1339649 (to B.D.). Supercomputer calculations were performed on Comet at the San Diego Supercomputing Center (support through an NSF/XSEDE grant TG-MCB070039N to B.D.) and on Lonestar-5 at the Texas Advanced Computing Center (supported through a UT grant TG457201 to B.D.). ITC experiments were performed using an ITC-200 microcalorimeter, funded by the NIH Shared Instrumentation Grant S10-OD017982. K.K.A.E. acknowledges the Bighley Graduate Student Fellowship. We thank Beckman Coulter, Indianapolis for the use of an Optima AUC instrument and for supporting this research financially. We thank Amy Henrickson for performing the CBZ/HPMCAS experiments at the Canadian Center for Hydrodynamics (University of Lethbridge, Alberta, Canada) with support from the Canada Foundation for Innovation (CFI-37589 to B.D.) and the Canada 150 Research Chairs program (C150-2017-00015 to B.D.). We also thank Dr. Courtney Aldrich for granting access to the ITC-200 microcalorimeter and Akash Bhattacharya and Amy Henrickson for their help with experimental runs.

REFERENCES

(1) Amidon, G. L.; Lennernäs, H.; Shah, V. P.; Crison, J. R. A Theoretical Basis for a Biopharmaceutic Drug Classification: The

Correlation of in Vitro Drug Product Dissolution and in Vivo Bioavailability. *Pharm. Res. An.* **1995**, *12*, 413−420.
(2) Babu, N. J.; Nangia, A. Solubility Advantage of Amorphous Drugs and Pharmaceutical Cocrystals. *Cryst. Growth Des.* **2011**, *11*, 2662−2679.
(3) Thayer, A. M. Finding Solutions. *Chem. Eng. News* **2010**, *88*, 13−18.
(4) Williams, H. D.; Trevaskis, N. L.; Charman, S. A.; Shanker, R. M.; Charman, W. N.; Pouton, C. W.; Porter, C. J. H. Strategies to Address Low Drug Solubility in Discovery and Development. *Pharmacol. Rev.* **2013**, *65*, 315−499.
(5) Leuner, C.; Dressman, J. Improving Drug Solubility for Oral Delivery Using Solid Dispersions. *Eur. J. Pharm. Biopharm.* **2000**, *50*, 47−60.
(6) Yuan, X.; Xiang, T.-X.; Anderson, B. D.; Munson, E. J. Hydrogen Bonding Interactions in Amorphous Indomethacin and Its Amorphous Solid Dispersions with Poly(Vinylpyrrolidone) and Poly(Vinylpyrrolidone-Co-Vinyl Acetate) Studied Using (13)C Solid-State NMR. *Mol. Pharmaceutics* **2015**, *12*, 4518−4528.
(7) Van Eerdenbrugh, B.; Taylor, L. S. Application of Mid-IR Spectroscopy for the Characterization of Pharmaceutical Systems. *Int. J. Pharm.* **2011**, *417*, 3−16.
(8) Mistry, P.; Mohapatra, S.; Gopinath, T.; Vogt, F. G.; Suryanarayanan, R. Role of the Strength of Drug−Polymer Interactions on the Molecular Mobility and Crystallization Inhibition in Ketoconazole Solid Dispersions. *Mol. Pharmaceutics* **2015**, *12*, 3339−3350.
(9) Alonzo, D. E.; Zhang, G. G. Z.; Zhou, D.; Gao, Y.; Taylor, L. S. Understanding the Behavior of Amorphous Pharmaceutical Systems during Dissolution. *Pharm. Res.* **2010**, *27*, 608−618.
(10) Friesen, D. T.; Shanker, R.; Crew, M.; Smithey, D. T.; Curatolo, W. J.; Nightingale, J. A. S. Hydroxypropyl Methylcellulose Acetate Succinate-Based Spray-Dried Dispersions: An Overview. *Mol. Pharmaceutics* **2008**, *5*, 1003−1019.
(11) Ueda, K.; Higashi, K.; Yamamoto, K.; Moribe, K. Inhibitory Effect of Hydroxypropyl Methylcellulose Acetate Succinate on Drug Recrystallization from a Supersaturated Solution Assessed Using Nuclear Magnetic Resonance Measurements. *Mol. Pharmaceutics* **2013**, *10*, 3801−3811.
(12) Kamerzell, T. J.; Esfandiary, R.; Joshi, S. B.; Middaugh, C. R.; Volkin, D. B. Protein−Excipient Interactions: Mechanisms and Biophysical Characterization Applied to Protein Formulation Development. *Adv. Drug Deliv. Rev.* **2011**, *63*, 1118−1159.
(13) Chen, Y.; Liu, C.; Chen, Z.; Su, C.; Hageman, M.; Hussain, M.; Haskell, R.; Stefanski, K.; Qian, F. Drug-Polymer-Water Interaction and Its Implication for the Dissolution Performance of Amorphous Solid Dispersions. *Mol. Pharmaceutics* **2015**, *12*, 576−589.
(14) Qiu, S.; Lai, J.; Guo, M.; Wang, K.; Lai, X.; Desai, U.; Juma, N.; Li, M. Role of Polymers in Solution and Tablet-Based Carbamazepine Cocrystal Formulations. *CrystEngComm* **2016**, *18*, 2664−2678.
(15) Marsac, P. J.; Rumondor, A. C. F.; Nivens, D. E.; Kestur, U. S.; Lia, S.; Taylor, L. S. Effect of Temperature and Moisture on the Miscibility of Amorphous Dispersions of Felodipine and Poly(Vinyl Pyrrolidone). *J. Pharm. Sci.* **2010**, *99*, 169−185.
(16) Macura, S.; Ernst, R. R. Elucidation of Cross Relaxation in Liquids by Two-Dimensional N.M.R. Spectroscopy. *Mol. Phys.* **2002**, *100*, 135−147.
(17) Hädener, M.; Gjuroski, I.; Furrer, J.; Vermathen, M. Interactions of Polyvinylpyrrolidone with Chlorin E6-Based Photosensitizers Studied by NMR and Electronic Absorption Spectroscopy. *J. Phys. Chem. B* **2015**, *119*, 12117−12128.
(18) Ting, J. M.; Tale, S.; Purchel, A. A.; Jones, S. D.; Widanapathirana, L.; Tolstyka, Z. P.; Guo, L.; Guillaudeu, S. J.; Bates, F. S.; Reineke, T. M. High-Throughput Excipient Discovery Enables Oral Delivery of Poorly Soluble Pharmaceuticals. *ACS Cent. Sci.* **2016**, *2*, 748−755.
(19) Cameron, K. S.; Fielding, L. NMR Diffusion Spectroscopy as a Measure of Host−Guest Complex Association Constants and as a Probe of Complex Size. *J. Org. Chem.* **2001**, *66*, 6891−6895.
(20) Fielding, L. Determination of Association Constants (Ka) from Solution NMR Data. *Tetrahedron* **2000**, *56*, 6151−6170.
(21) Cohen, Y.; Avram, L.; Frish, L. Diffusion NMR Spectroscopy in Supramolecular and Combinatorial Chemistry: An Old Parameter-New Insights. *Angew. Chem., Int. Ed.* **2005**, *44*, 520−554.
(22) Li, Z.; Johnson, L. M.; Ricarte, R. G.; Yao, L. J.; Hillmyer, M. A.; Bates, F. S.; Lodge, T. P. Enhanced Performance of Blended Polymer Excipients in Delivering a Hydrophobic Drug through the Synergistic Action of Micelles and HPMCAS. *Langmuir* **2017**, *33*, 2837−2848.
(23) Lee, J. H.; Okuno, Y.; Cavagnero, S. Sensitivity Enhancement in Solution NMR: Emerging Ideas and New Frontiers. *J. Magn. Reson.* **2014**, *241*, 18−31.
(24) Freyer, M. W.; Lewis, E. A. Isothermal Titration Calorimetry: Experimental Design, Data Analysis, and Probing Macromolecule/Ligand Binding and Kinetic Interactions. *Methods Cell Biol.* **2008**, *84*, 79−113.
(25) Meng, F.; Jing, Z.; Ferreira, R.; Ren, P.; Zhang, F. Investigating the Association Mechanism between Rafoxanide and Povidone. *Langmuir* **2018**, *34*, 13971−13978.
(26) Bekdemir, A.; Stellacci, F. A Centrifugation-Based Physicochemical Characterization Method for the Interaction between Proteins and Nanoparticles. *Nat. Commun.* **2016**, *7*, 1−8.
(27) Salveson, P. J.; Haerianardakani, S.; Thuy-Boun, A.; Yoo, S.; Kreutzer, A. G.; Demeler, B.; Nowick, J. S. Repurposing Triphenylmethane Dyes to Bind to Trimers Derived from Aβ. *J. Am. Chem. Soc.* **2018**, *140*, 11745−11754.
(28) Karabudak, E.; Brookes, E.; Lesnyak, V.; Gaponik, N.; Eychmüller, A.; Walter, J.; Segets, D.; Peukert, W.; Wohlleben, W.; Demeler, B.; et al. Simultaneous Identification of Spectral Properties and Sizes of Multiple Particles in Solution with Subnanometer Resolution. *Angew. Chem., Int. Ed.* **2016**, *55*, 11770−11774.
(29) Demeler, B.; Van Holde, K. E. Sedimentation Velocity Analysis of Highly Heterogeneous Systems. *Anal. Biochem.* **2004**, *335*, 279−288.
(30) Maechtle, W.; Borger, L. *Analytical Ultracentrifugation of Polymers and Nanoparticles*; Springer Laboratory; Springer-Verlag: New York, 2006. DOI: 10.1007/b137083.
(31) Raşa, M.; Schubert, U. S. Progress in the Characterization of Synthetic (Supramolecular) Polymers by Analytical Ultracentrifugation. *Soft Matter* **2006**, *2*, 561−572.
(32) Mistry, P.; Amponsah-Efah, K. K.; Suryanarayanan, R. Rapid Assessment of the Physical Stability of Amorphous Solid Dispersions. *Cryst. Growth Des.* **2017**, *17*, 2478−2485.
(33) Mistry, P.; Suryanarayanan, R. Strength of Drug−Polymer Interactions: Implications for Crystallization in Dispersions. *Cryst. Growth Des.* **2016**, *16*, 5141−5149.
(34) Amponsah-Efah, K. K.; Mistry, P.; Eisenhart, R.; Suryanarayanan, R. The Influence of Drug-Polymer Interactions on the Dissolution Performance of Amorphous Solid Dispersions. *Mol. Pharmaceutics* (in press)
(35) Amponsah-Efah, K. K.; Mistry, P.; Eisenhart, R.; Suryanarayanan, R. *The Influence of Drug-Polymer Interactions on the Dissolution Performance of Amorphous Solid Dispersions*. In Published abstract, Amercian Association of Pharmaceutical Scientists (AAPS) Annual Meeting; 2017.
(36) Shamma, R. N.; Basha, M. Soluplus: A Novel Polymeric Solubilizer for Optimization of Carvedilol Solid Dispersions: Formulation Design and Effect of Method of Preparation. *Powder Technol.* **2013**, *237*, 406−414.
(37) BASF. *Soluplus-Technical Information*. No. 03_090801e-04 , 1−8.
(38) Curatolo, W.; Nightingale, J. A.; Herbig, S. M. Utility of Hydroxypropylmethylcellulose Acetate Succinate (HPMCAS) for Initiation and Maintenance of Drug Supersaturation in the GI Milieu. *Pharm. Res.* **2009**, *26*, 1419−1431.
(39) Ishizuka, Y.; Ueda, K.; Okada, H.; Takeda, J.; Karashima, M.; Yazawa, K.; Higashi, K.; Kawakami, K.; Ikeda, Y.; Moribe, K. Effect of Drug-Polymer Interactions through Hypromellose Acetate Succinate

https://dx.doi.org/10.1021/acs.molpharmaceut.0c00849
Mol. Pharmaceutics XXXX, XXX, XXX−XXX

Substituents on the Physical Stability on Solid Dispersions Studied by Fourier-Transform Infrared and Solid-State Nuclear Magnetic Resonance. *Mol. Pharmaceutics* **2019**, *16*, 2785−2794.
(40) Ueda, K.; Higashi, K.; Yamamoto, K.; Moribe, K. The Effect of HPMCAS Functional Groups on Drug Crystallization from the Supersaturated State and Dissolution Improvement. *Int. J. Pharm.* **2014**, *464*, 205−213.
(41) Fukasawa, M.; Obara, S. Molecular Weight Determination of Hypromellose Acetate Succinate (HPMCAS) Using Size Exclusion Chromatography with a Multi-Angle Laser Light Scattering Detector. *Chem. Pharm. Bull. (Tokyo)* **2004**, *52*, 1391−1393.
(42) Demeler, B.. UltraScan: A Comprehensive Data Analysis Software Package for Analytical Ultracentrifugation Experiments. In *Modern Analytical Ultracentrifugation: Techniques and Methods*; Scott, D. J., Harding, S. E., Rowe, A. J., Eds.; Royal Society of Chemistry, 2005; 210−230. DOI: 10.1039/9781847552617-00210.
(43) Demeler, B.; Gorbet, G. E. Analytical Ultracentrifugation Data Analysis with UltraScan-III. In *Analytical Ultracentrifugation*; Springer Japan: Tokyo, 2016; 119−143. DOI: 10.1007/978-4-431-55985-6_8.
(44) Brookes, E.; Cao, W.; Demeler, B. A Two-Dimensional Spectrum Analysis for Sedimentation Velocity Experiments of Mixtures with Heterogeneity in Molecular Weight and Shape. *Eur. Biophys. J.* **2010**, *39*, 405−414.
(45) Demeler, B.; Brookes, E. Monte Carlo Analysis of Sedimentation Experiments. *Colloid Polym. Sci.* **2008**, *286*, 129−137.
(46) Gorbet, G.; Devlin, T.; Hernandez Uribe, B. I.; Demeler, A. K.; Lindsey, Z. L.; Ganji, S.; Breton, S.; Weise-Cross, L.; Lafer, E. M.; Brookes, E. H.; et al. A Parametrically Constrained Optimization Method for Fitting Sedimentation Velocity Experiments. *Biophys. J.* **2014**, *106*, 1741−1750.
(47) Demeler, B.; Saber, H. Determination of Molecular Parameters by Fitting Sedimentation Data to Finite-Element Solutions of the Lamm Equation. *Biophys. J.* **1998**, *74*, 444−454.
(48) Piñeiro, Á.; Muñoz, E.; Sabín, J.; Costas, M.; Bastos, M.; Velázquez-Campoy, A.; Garrido, P. F.; Dumas, P.; Ennifar, E.; García-Río, L.; et al. AFFINImeter: A Software to Analyze Molecular Recognition Processes from Experimental Data. *Anal. Biochem.* **2019**, *577*, 117−134.
(49) Swift, T.; Swanson, L.; Geoghegan, M.; Rimmer, S. The PH-Responsive Behaviour of Poly(Acrylic Acid) in Aqueous Solution Is Dependent on Molar Mass. *Soft Matter* **2016**, *12*, 2542−2549.
(50) Berkowitz, S. A.; Philo, J. S.. Characterizing Biopharmaceuticals Using Analytical Ultracentrifugation. In *Biophysical Characterization of Proteins in Developing Biopharmaceuticals*; Elsevier, 2015; 211−260. DOI: 10.1016/B978-0-444-59573-7.00009-9.
(51) Stafford, W. F. Analysis of Nonideal, Interacting, and Noninteracting Systems by Sedimentation Velocity Analytical Ultracentrifugation. In *Analytical Ultracentrifugation*; Springer Japan: Tokyo, 2016; 463−482. DOI: 10.1007/978-4-431-55985-6_23.
(52) Chaturvedi, S. K.; Sagar, V.; Zhao, H.; Wistow, G.; Schuck, P. Measuring Ultra-Weak Protein Self-Association by Non-Ideal Sedimentation Velocity. *J. Am. Chem. Soc.* **2019**, *141*, 2990−2996.
(53) Ricarte, R. G.; Li, Z.; Johnson, L. M.; Ting, J. M.; Reineke, T. M.; Bates, F. S.; Hillmyer, M. A.; Lodge, T. P. Direct Observation of Nanostructures during Aqueous Dissolution of Polymer/Drug Particles. *Macromolecules* **2017**, *50*, 3143−3152.
(54) Zhang, J.; Pearson, J. Z.; Gorbet, G. E.; Cölfen, H.; Germann, M. W.; Brinton, M. A.; Demeler, B. Spectral and Hydrodynamic Analysis of West Nile Virus RNA−Protein Interactions by Multi-wavelength Sedimentation Velocity in the Analytical Ultracentrifuge. *Anal. Chem.* **2017**, *89*, 862−870.
(55) Dressman, J. B.; Reppas, C. In Vitro-in Vivo Correlations for Lipophilic, Poorly Water-Soluble Drugs. *Eur. J. Pharm. Sci.* **2000**, *11*, S73−S80.
(56) Turnbull, W. B.; Daranas, A. H. On the Value of *c* : Can Low Affinity Systems Be Studied by Isothermal Titration Calorimetry? *J. Am. Chem. Soc.* **2003**, *125*, 14859−14866.
(57) Murphy, D.; Rodriguez-Cintrón, F.; Langevin, B.; Kelly, R.; Rodriguez-Hornedo, N. Solution-Mediated Phase Transformation of Anhydrous to Dihydrate Carbamazepine and the Effect of Lattice Disorder. *Int. J. Pharm.* **2002**, *246*, 121−134.
(58) Craig, D. Q. The Mechanisms of Drug Release from Solid Dispersions in Water-Soluble Polymers. *Int. J. Pharm.* **2002**, *231*, 131−144.
(59) Sun, D. D.; Lee, P. I. Probing the Mechanisms of Drug Release from Amorphous Solid Dispersions in Medium-Soluble and Medium-Insoluble Carriers. *J. Control. Release* **2015**, *211*, 85−93.
(60) Sun, D. D.; Lee, P. I. Evolution of Supersaturation of Amorphous Pharmaceuticals: The Effect of Rate of Supersaturation Generation. *Mol. Pharmaceutics* **2013**, *10*, 4330−4346.
(61) Fung, M.; Bērziņš, K.; Suryanarayanan, R. Physical Stability and Dissolution Behavior of Ketoconazole−Organic Acid Coamorphous Systems. *Mol. Pharmaceutics* **2018**, *15*, 1862−1869.

https://dx.doi.org/10.1021/acs.molpharmaceut.0c00849
Mol. Pharmaceutics XXXX, XXX, XXX−XXX